# Bridge Damage detection using ambient traffic and Moving Force Identification

**OBrien, E.J., Carey, C., Keenahan, J.**

## 1. Introduction

In most developed countries, bridge condition is assessed based on visual inspections. Such inspections are, however, labour intensive and often an unreliable way of determining the true condition. Examples of the importance of effective bridge inspection include the collapse of the Interstate 34 Bridge in Minneapolis on 1st August 2007 [1] and the collapse of an Interstate 5 bridge over the Skagit River in Seattle on 27th May 2012 [2]. In other cases, over-precautionary measures are taken and unnecessary repairs result. The shortcomings of visual inspections, combined with the increase in computational power and signal processing capacity have resulted in a move towards sensor based monitoring of bridge condition in recent years. A brief literature review is provided here into damage detection methods for bridges. More comprehensive literature reviews can be found in [[3]–[6]].

The physically tangible relation between changes in stiffness or mass and changes in natural frequency has led many in the field of damage detection to use natural frequency as an indicator of damage [7]. Cerda et al. [8] carry out experimental work where damage is simulated as a change in bridge mass, and changes in frequency are tested as the damage indicator. Messina et al. [9] present a method based on linearized shifts in frequency due to damage and considers changes in stiffness only, capable of tackling multiple damage locations and intensities.

A damage detection algorithm, where information on the location and severity of damage is inferred directly from changes in mode shapes, is presented by Kim & Stubbs [10]. In an effort to compare frequency and mode shape methods, Kim et al. [11] applied both a frequency based and a modal strain energy based method to identify damage location and severity in a simulated beam. The two methods are used for several damage scenarios and it is found that the modal strain energy method gives a more accurate prediction of location than the frequency based method. It may be difficult however to detect the difference in modal characteristics between healthy and slightly damaged structures to the required level of accuracy in the field. Shih et al. [12] recommend a combination of change in natural frequency, modal stain energy and modal flexibility in their damage detection methodology.

Compared with mode shapes and natural frequencies, there has been less research on the use of damping as a damage indicator [13]. It is believed, however, that in some cases damping is more sensitive than natural frequencies [14]. Curadelli et al. [15] show that in certain cases, little or no frequency change is detected but that changes in damping are successfully used to detect cracks. Modena et al. [16] show that some

cracks cause significant changes in damping but cause very little change in frequency and need higher mode shapes to be detected. Jeary et al. [17] extract non-linear damping data from short time histories of the response of thirty structures to random vibration and discuss the possibility of changes in damping being an indicator of bridge damage. Further, many researchers note that damping can be a useful damage sensitive feature and is highly indicative of the amount of damage that a structure has undergone during its lifetime [18]–[20].

Wavelet transforms can be used to accentuate discontinuities in a signal such as the discontinuity of slope when an axle passes over a damaged section. They are based on the idea that any signal can be broken down into a series of local basis functions called wavelets. The transform may be applied and mapped to the space or time domain of the structure. Thus, they may be used to find an abrupt change in a mode shape [21]–[23], often indicative of damage, locate a sudden change in response from an acceleration time response [24] and [25], or analyse the displacement response at the mid-span of a bridge [26]. In each case, the energy of the abnormal signal indicates the size of the crack.

A neural network is a numerical technique to relate outputs to inputs. It consists of an interconnected group of processing units known as neurons. It is most often an adaptive system that changes its structure during a training phase. The trained network is used to model complex relationships between inputs and outputs, and to find patterns in data. They have been applied successfully in many diverse applications including vibration-based damage identification. In general, neural networks are applicable to problems where a significant database of information is available, but where it is difficult to specify an explicit relationship. Hattori et al. [27] develop a bridge condition identification technique based on a Neural Network technique. The running vehicle-induced bridge vibration data is the input and the structural damage condition is the output. Lee et al. [28] present a neural network-based damage detection method using differences in mode shapes between healthy and damaged structures as the basic feature for damage detection.

This paper describes a novel approach that uses a Moving Force Identification (MFI) algorithm to indicate deterioration of the bridge's condition. The application of MFI to health monitoring was proposed by OBrien et al. [29] wherein an instrumented vehicle is used for drive by inspections. This paper uses the mean force estimate for individual axles of a population of vehicles crossing a bridge to detect damage at relatively low levels. The vehicle parameters used to generate the forces measured come from Weigh-in-Motion (WIM) data from a fleet of 2-axle vehicles and so the damage is detected using ambient traffic as in [30]. The underlying reasons for the method's effectiveness are first explained using static equations. Various MFI techniques are then introduced with the specific MFI theory used in this text explained in detail in Section 3. Section 5 discusses the shortcomings of using strain signals and the need to use deflection data to detect damage [31].

## 2. Static concept - how damage affects calculated force

Beam deflections, *d*, resulting from two moving point loads (60 kN and 80 kN), are found using the principle of virtual work. The two point forces, 4 m apart, are simulated at 2 m intervals crossing a 24 m simply supported beam (Fig. 1). The Modulus of Elasticity of the beam is taken as $E = 35 \times 10^9$ N m$^{-2}$ and the second moment of area is taken as $I = 0.5$ m$^4$.

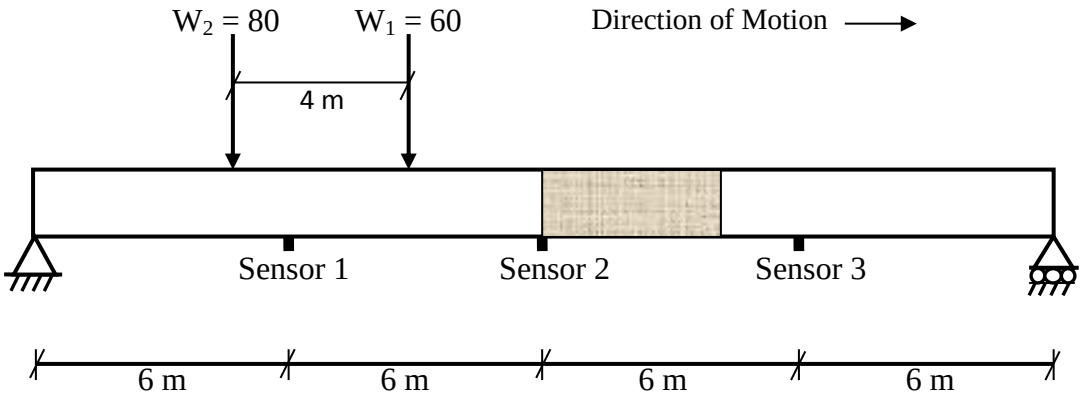


Figure 1: Two point forces traversing a simply supported beam

A displacement history of the beam is calculated at the three sensor locations shown in Fig. 1 (quarter span, mid span and three quarter span). This is repeated for a beam containing damage where damage is modelled as a reduction in bending stiffness (levels used are 5%, 15% and 30%) and the affected portion of the beam begins at mid span and ends 4 m to the right. The history of total deflection for the sensor at mid span, for these levels of damage is illustrated in Fig. 2. As expected, deflection increases as the beam becomes increasingly damaged.

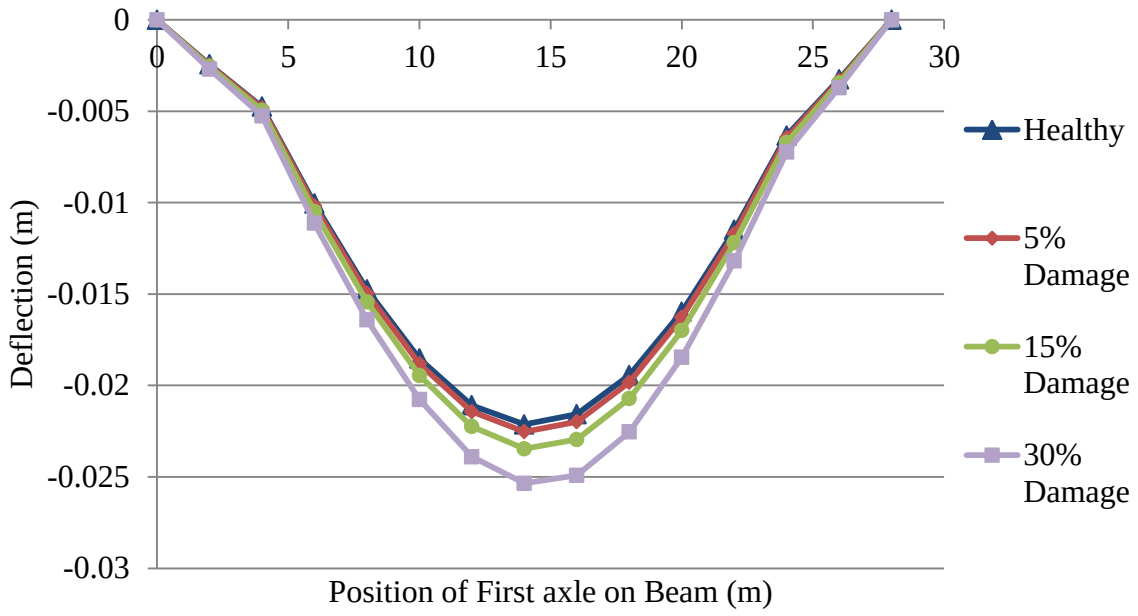


Figure 2: Deflections at mid span due to two point loads for varying levels of damage

An optimisation approach is considered for damage detection where an objective function is formulated, equal to the sum of the squares of the differences between measured and theoretical deflections at the three sensor locations. The theoretical deflections are always taken as the healthy deflections and the measured deflections may be healthy or damaged. The objective function for the $i^{th}$ scan is:

$$O_i = \left(d_{1i}^{Me} - d_{1i}^{Th}\right)^2 + \left(d_{2i}^{Me} - d_{2i}^{Th}\right)^2 + \left(d_{3i}^{Me} - d_{3i}^{Th}\right)^2 \quad (1)$$

where $d_{si}^{Th}$ is the theoretical deflection at sensor $s$ for scan $i$ and $d_{si}^{Me}$ is the corresponding measured value. The forces that minimise this objective function are found by taking partial derivatives with respect to $W_1$ and $W_2$. This is similar to the traditional approach to Bridge Weigh-in-Motion (BWIM) first proposed by Moses [32] and further described by OBrien [33], [34]:

$$\frac{\partial O_i}{\partial \mathrm{W}_j} = 2\left(d_{1i}^{Me} - d_{1i}^{Th}\right)\left(\frac{\partial\left(-d_{1i}^{Th}\right)}{\partial \mathrm{W}_j}\right) + 2\left(d_{2i}^{Me} - d_{2i}^{Th}\right)\left(\frac{\partial\left(-d_{2i}^{Th}\right)}{\partial \mathrm{W}_j}\right) + 2\left(d_{3i}^{Me} - d_{3i}^{Th}\right)\left(\frac{\partial\left(-d_{3i}^{Th}\right)}{\partial \mathrm{W}_j}\right) \quad for\ j = 1,2 \quad (2)$$

Setting both derivatives to zero gives two equations in two unknowns for each scan, $i$, allowing the two forces to be calculated. For the case of a healthy bridge, the measured deflections are the same as the theoretical ones, so the calculated forces are the same as the applied forces and are constant for all $i$. If a bridge is damaged the measured deflections increase. If the forces are then calculated assuming a healthy

bridge, this results in errors in the calculated values. The calculated forces for varying levels of damage are given in Fig. 3.

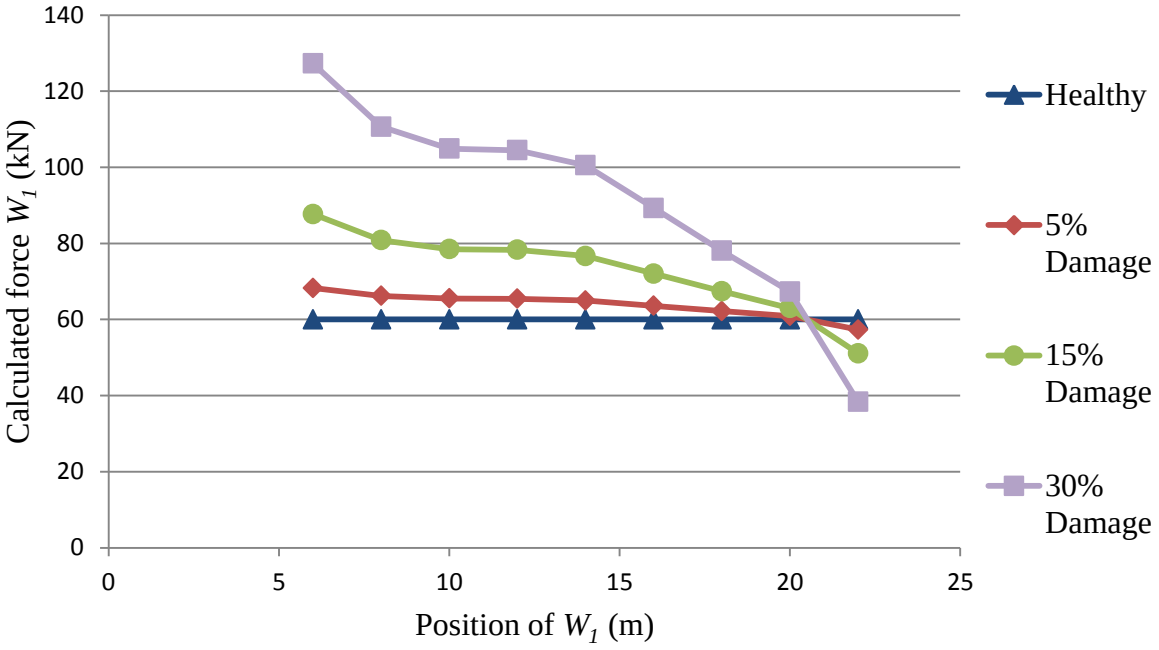


(a): Calculated force, $W_1$

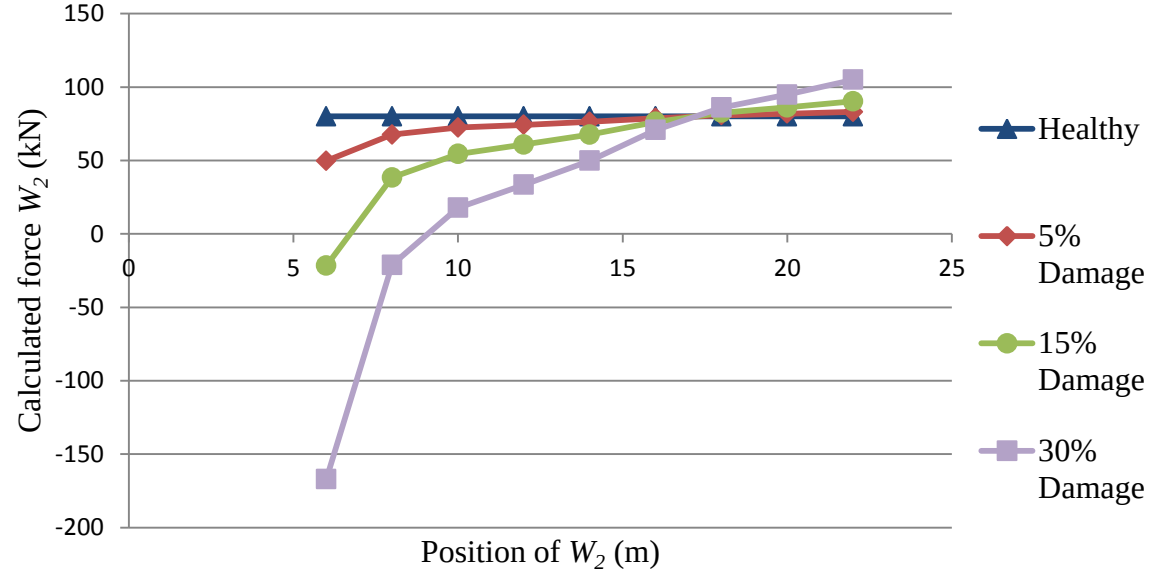


(b): Calculated force, $W_2$

Figure 3: Calculated forces for varying levels of damage

Fig. 3 shows that the algorithm correctly predicts the forces in the case of a healthy beam but is sensitive to damage. The determinant of the system of equations is near zero, confirming that the system of equations is not well-conditioned. This has the effect of amplifying the sensitivity of the results to local losses of stiffness.

## 3. Dynamic concept – MFI theory for damage detection

In MFI, a forcing function is sought for the dynamic equations such that the difference between what is measured and what is calculated is at a minimum. General reviews of MFI theory can be found in [35] and [36]. The MFI method used in this paper is referred to as the Optimal State Estimation Approach [37], where the minimisation is treated as a multi-dimensional control process using dynamic programming. The method was first proposed by Law and Fang [37] and subsequently improved upon by González et al. [34]. The second order matrix differential equation for structural dynamics is:

$$[M_g]\left\{\frac{d^2u}{dt^2}\right\} + [C_g]\left\{\frac{du}{dt}\right\} + [K_g]\{u\} = F(t) \tag{3}$$

where $\{u\}$ is the vector of displacements, $M_g$, $C_g$ and $K_g$ are the mass, damping and stiffness matrices respectively and $F(t)$ is the vector of forcing functions. Eq. 3 is reduced from a second order equation to two first order equations by defining the state variables of velocity $\{v\}$ and acceleration $\{a\}$ :

$$\{v\} = \left\{\frac{du}{dt}\right\} \tag{4}$$

$$\{a\} = \left\{\frac{dv}{dt}\right\} = -[M_g]^{-1}[C_g]\{v\} - [M_g]^{-1}[K_g]\{u\} + [M_g]^{-1}[L]\{g(t)\} \tag{5}$$

where $[L]$ is the location matrix which distributes the forcing function $\{g(t)\}$ to the relevant degrees of freedom. Eq. 4 and Eq. 5 are combined in matrix form to give:

$$\frac{d}{dt}\begin{Bmatrix} u \\ v \end{Bmatrix} = \begin{bmatrix} 0 & I \\ -[M_g]^{-1}[K_g] & -[M_g]^{-1}[C_g] \end{bmatrix}\begin{Bmatrix} u \\ v \end{Bmatrix} + \begin{bmatrix} 0 \\ [M_g]^{-1}[L] \end{bmatrix}\{g(t)\} \tag{6}$$

which is then rewritten using the state vector $\{X\}$ which contains the state variables $\{u\}$ and {v}:

$$\frac{d\{X\}}{dt} = [A]\{X\} + f(t) \tag{7}$$

Eq. 7 is converted into a discrete time integration scheme using Laplace Transforms, the Exponential matrix and Padé approximations [38] and becomes:

$$\{X\}_{j+1} = [M]\{X\}_j + [P]\{g\}_j \tag{8}$$

where

$$[\mathrm{P}] = [M - I][A]^{-1}\begin{bmatrix} 0 \\ [M_g]^{-1}[L] \end{bmatrix} \tag{9}$$

and

$$M = \mathrm{e}^{[\mathbf{A}]\mathrm{h}} \tag{10}$$

where $h$ is the time step between consecutive points $j$ and $j$+1. The measurements, $d_j$, are taken at discrete points on the bridge and so a matrix, $Q$, must be used to relate the measurements to the relevant state variables. The optimisation is then to find $\{g\}_j$ that minimises the error given by,

$$E(X_j, g_j) = \sum_{j=1}^{N} \left( (QX_j - d_j), W(QX_j - d_j) \right) + (g_j, Bg_j) \tag{11}$$

subject to Eq. 8 and where $(x, y)$ denotes the vector product and $W$ is the identity matrix. This inverse problem is highly ill-conditioned and so a regularisation parameter is introduced that solves a nearby problem and improves the conditioning of the system. $B$ is a diagonal matrix of the regularisation parameter and the number of terms of $B$ is dependent on the number of axles. The optimal regularisation parameter is chosen using the L-curve method [39]. The L-curve is a plot of the smoothing norm of the regularised solution versus the residual norm of the error on a log-log scale and the optimal parameter is chosen from the corner of the L shape. This paper utilizes first order regularisation [[34]] in which the derivative of the force is regularised and the force vector is then included in the state vector.

The minimisation problem is solved using dynamic programming [40] and Bellman's principle of optimality [41]. Eq. 11 is known as a policy function and the optimal policy is that which minimises the overall error of the process. The optimal forcing function is found through a backward and forward loop. In this paper the forcing function found using MFI theory is shown to be highly sensitive to bridge damage.

## 4. Vehicle – bridge interaction modelling

A bridge example is used to illustrate the damage detection approach. The simply supported bridge is modelled using 24 1 m beam long finite elements, each with two nodes and two degrees of freedom per node. The depth of the beam is 1.2 m and the second moment of area and cross sectional area are 1.152 $m^4$ and 10 $m^2$ respectively. The Young's Modulus is 35 × $10^9$ N $m^{-2}$ and the density is 2400 kg $m^{-3}$. The bridge damping ratio is taken as 3%. Damage is modelled as recommended by Sinha et al. [42] and used in [24], [43]–[45] where a crack causes a loss in stiffness over a region

of three times the beam depth, varying linearly from a maximum at the centre. Fig. 4 illustrates a crack at element fourteen of the beam, 2 m right of mid-span. A damage parameter, $\delta$, is defined as the ratio of crack depth to overall beam depth; thus $\delta$ = 0.25 implies that the crack depth is 25% of the beam depth.

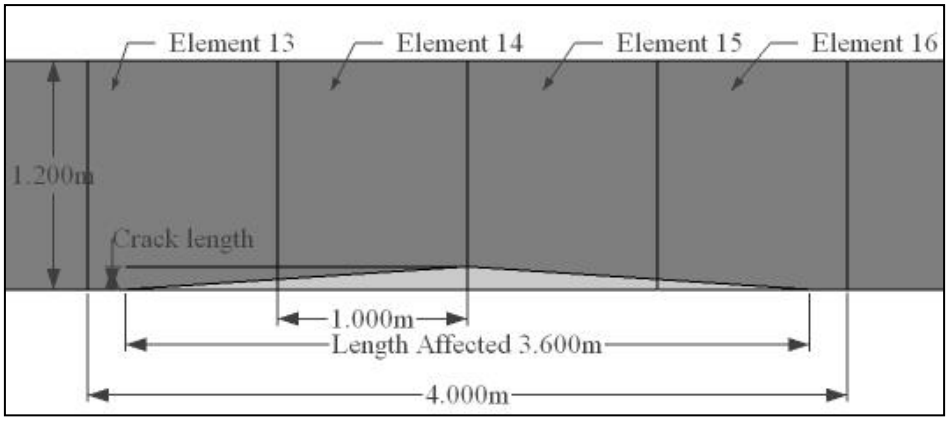


Figure 4: Damage location and extent

The road profile used is generated according to ISO Class 'A' [46], i.e. 'very good'. Adjacent road profiles are correlated and this creates a three dimensional ‘carpet’ profile [47]. Fig. 5 shows a 50 m section of road profile with all possible wheel paths highlighted. This profile is passed through a moving average filter of length 0.24 m in order to take into account the tyre contact patch. The transverse positions of the vehicles are generated using Monte Carlo simulation assuming a truncated normal distribution with a mean path 2 m from the edge.

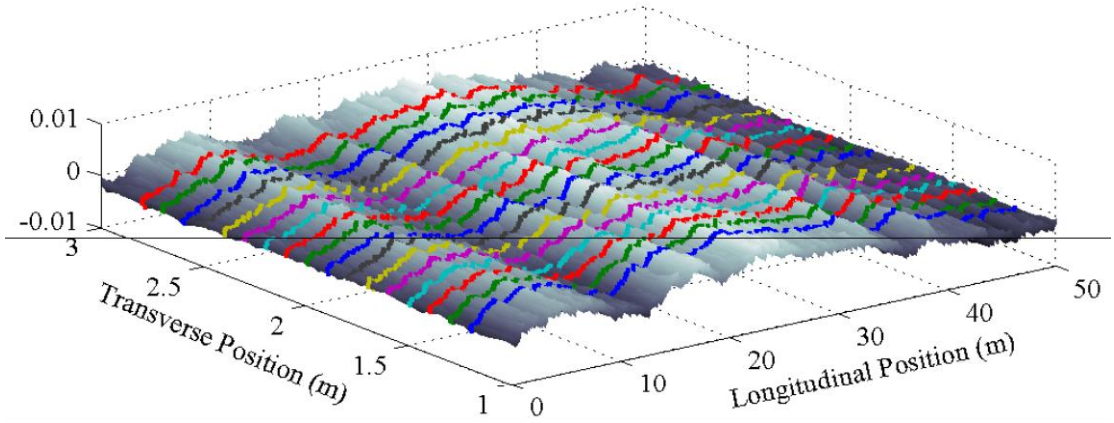


Figure 5: Road profile section with highlight of possible paths

The fleet of vehicles consists of 2-axle 'Half-Car' models which take into account axle-hop, pitch and bounce degrees of freedom. The properties for the static axle weights, the vehicle speed and the distance between axles is taken from a WIM site at Arnhem in the Netherlands. A database of 128,604 2-axle trucks with axle spacings between 4 m and 6 m, was extracted from the general traffic data. The properties illustrated in Fig. 6 are taken from this database.

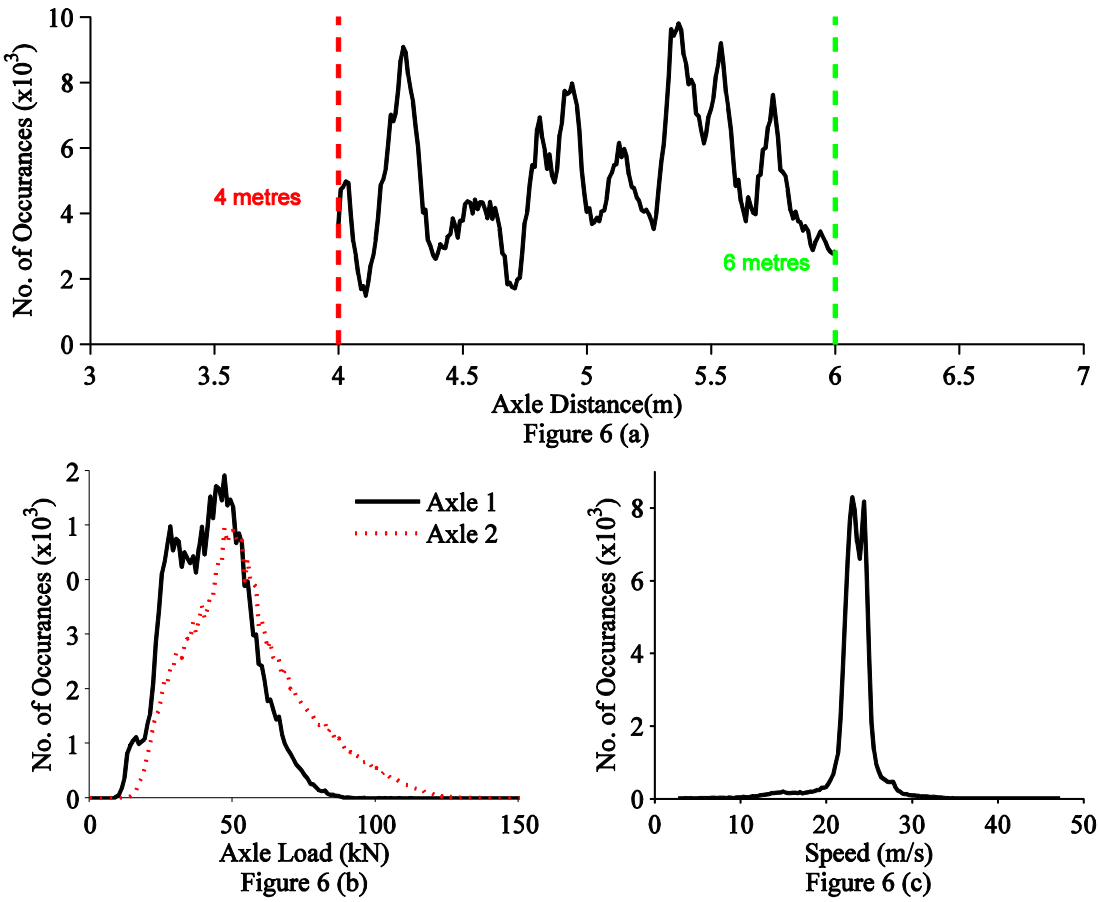


Figure 6: Histograms of vehicle properties (a) Axle spacing (b) Axle weights (c) Vehicle speed

Mean and standard deviation values for unsprung mass, suspension stiffness, suspension damping and tyre stiffness parameters are taken from [48], [49], and are shown in Table 1.

Table 1: Dynamic properties of vehicle fleet

| | Mean Value | Standard deviation | Minimum | Maximum | Unit |
|---|---|---|---|---|---|
| Unsprung Mass | 750 | 250 | 500 | 1000 | Kg |
| Suspension Stiffness | 750000 | 250000 | 500000 | 1000000 | N/m |
| Suspension Damping | 10000 | 2500 | 5000 | 15000 | N s/m |
| Tyre Stiffness | 3500000 | 1000000 | 2000000 | 5000000 | N/m |

## 5. MFI and damage detection using strains

In general BWIM applications [33], [50], [51],bridge strains are used to infer axle weights. A population of 1000 vehicles is simulated crossing the 24 m long beam. White Gaussian noise with a signal to noise ratio of 50 is added to the strains to allow for measurement error. More severe signal to noise ratios would, of course, affect the accuracy of the MFI. The inferred forces are calculated using strain signals from measurement points on the bridge at 6 m, 12 m and 18 m (the quarter, mid, and three

quarter spans respectively). The mean force for the 1000 vehicles is found and this produces a force pattern which can be compared to further batches of vehicles crossing the same profile, due to statistical spatial repeatability (SSR) [52] which averages out the effect of individual vehicle dynamics. The resulting inferred forces are seen in Fig. 7 for four different conditions: (1) a healthy beam, (2) crack at mid-span, (3) crack 1 m right of mid-span and (4) crack 2 m right of mid-span. In all three cases containing cracks, a level of damage of $\delta = 0.3$ is assumed.

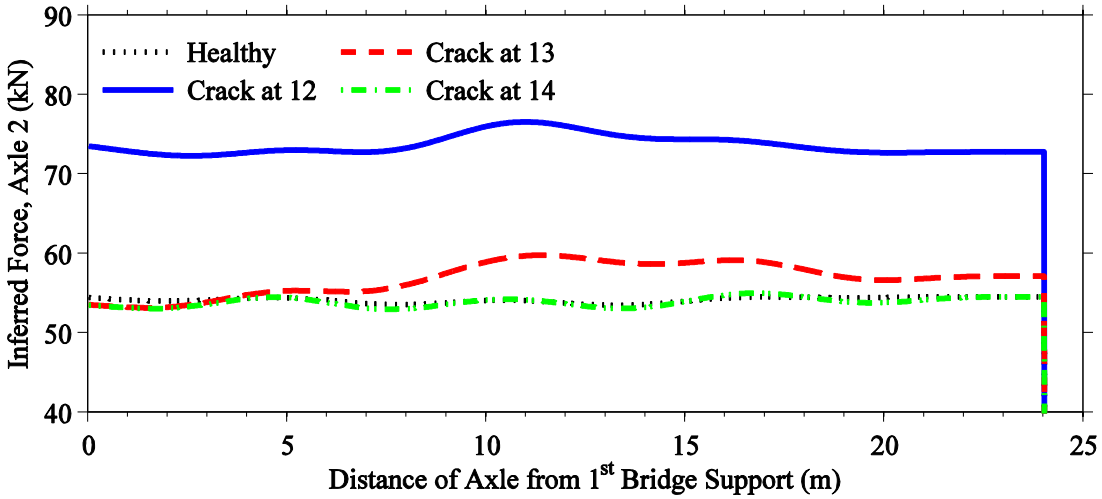


Figure 7: Axle forces inferred using strains (12 = mid-span; 13 & 14 = 1m and 2m right of mid-span respectively)

The crack at mid-span is directly at a sensor location so the effect is significant. However, once the distance between the sensor and the damage location becomes greater than the triangular extent of stiffness loss (2m right of mid-span), the damage can no longer be detected. As the beam is statically determinant, the stress distribution is independent of all element stiffness and the stress is only affected by a loss of stiffness at the sensor location. Yao et al [53] make note of this need for strain sensors to be in direct contact with affected areas in their review of crack detection techniques. It can be noted that predicted forces for the healthy case and those where the crack is 2 m right of mid-span are not quite identical. This is due to the differing transverse positions at which the vehicles travel across the carpet profile. It is concluded that strains in a determinant structure are of limited value in terms of damage detection.

## 6. MFI and damage detection using deflections

To overcome this issue, deflection is assumed to be measured at the three measurement points instead of strain. Camera technologies are improving rapidly and it is reasonable to assume that deflections can soon be measured accurately using a camera at a high scanning frequency. Wu and Casciati [54] provide an overview for non-contact sensor detection of displacements and RaghuPrasad et al. [55] discuss using static deflection measurements as a means of damage detection. Recent use of

deflections measurements in moving load prediction can be seen in [56], [57]. Deflections are calculated here using the Newmark-β integration scheme [58] and the vehicle-bridge dynamic interaction is then solved iteratively as described by Green and Cebon [59]. As with the strain signals, Gaussian white noise with a signal to noise ratio of 50 is added to the calculated deflections to allow for measurement error. A population of 1000 2-axle vehicles generated using the properties of Figure 6 and Table 1 were simulated crossing the 24 m span simply supported beam. This process is first completed on a healthy bridge. For each vehicle, MFI is used to infer the axle force from the measured deflection. Cracks are then introduced to the bridge models using damage levels of $\delta = 0.05$, $\delta = 0.15$ and $\delta = 0.30$. All damage is taken to occur 2 m right of mid-span (i.e. at the 14$^{th}$ element). For each level of damage the procedure is carried out for two samples of 1000 vehicles to show the degree of repeatability.

The inferred axle force patterns for the front and rear axles are shown in Fig. 8 for the healthy case, and for the three different levels of damage. Each curve represents the mean of 1000 inferred force histories.

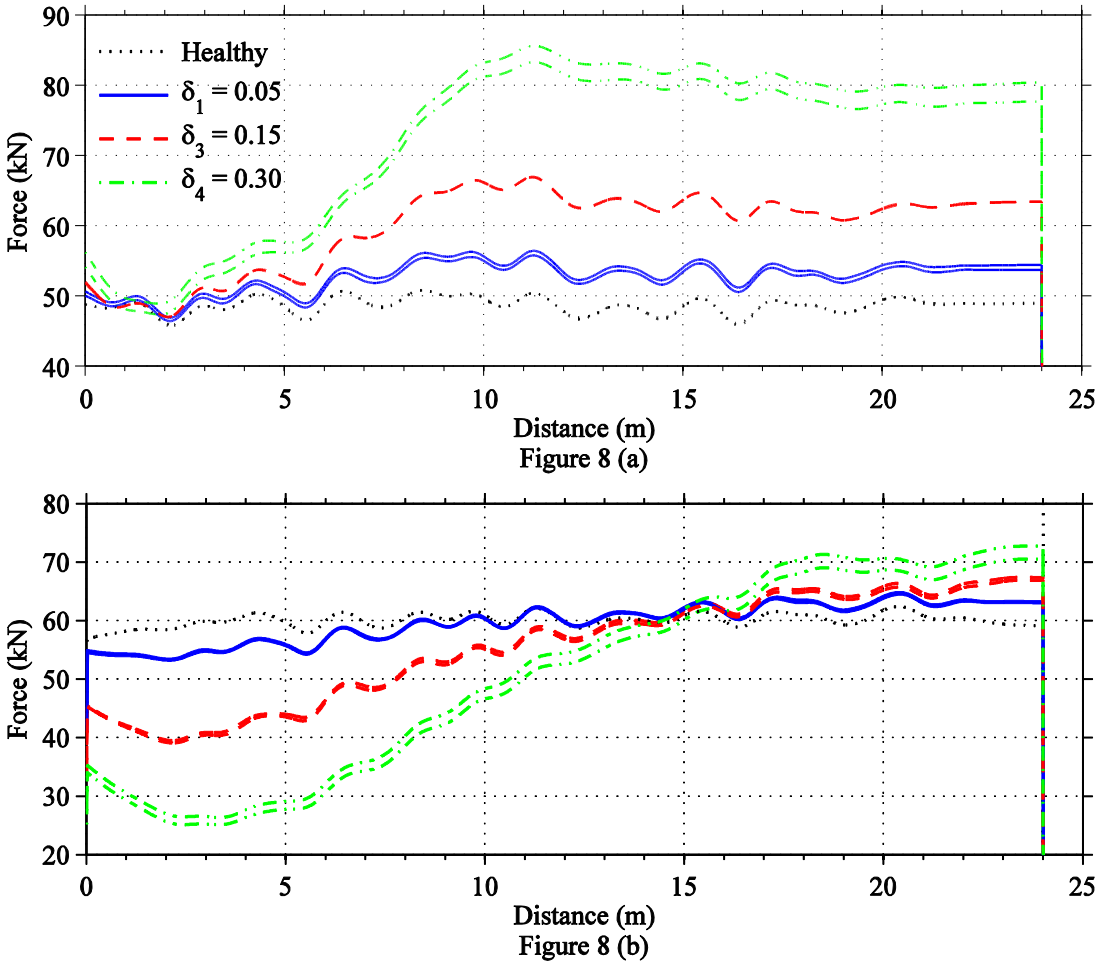


Figure 8: Mean of 1000 inferred axle force histories using deflection measurements from a bridge with vary degrees of damage (a) Axle 1 (b) Axle 2

Fig. 8 confirms that the mean inferred force pattern is highly sensitive to damage in the bridge. It is important to note that this damage indication requires no knowledge of the two-axle vehicle fleet. The change is related to the damage level with the deviation from the healthy bridge condition increasing with increased damage, although not proportionately. The results of the inferred forces of the first axle appear intuitive. Damage leads to an increase in deflection and the MFI, not knowing about the damage, over-predicts the force. The ability of the inferred force to indicate damage on the bridge is at its worst, in terms of detecting damage, when the axle is alone on the bridge before the arrival of the second axle (4-6 m later). The results of the inferred forces of the second axle show a somewhat similar trend to the first axle. Damage leads to an increase in deflection and the MFI, again, over-predicts the force. Similar to the first axle, the ability of the inferred force to indicate damage on the bridge is at its best when both axles are on the bridge, and at its worst when the first axle leaves the bridge (4-6 m earlier).

The results show good repeatability with the force history estimation for each pair of runs staying reasonably close to each other. The repeatability would clearly improve for large samples of similar vehicles.

## 7. Influence of damage location and extent

To investigate how the location of the decreased stiffness affected damage identification, a study was carried out in which 100 batches of 100 vehicles crossed the 24 m bridge with δ randomly varying between 0.01 and 0.30 for each batch. The location of the damage also varied randomly from 3-21 m. The indicator used to quantify the difference from a healthy bridge scenario was the root mean square of the differences between the mean inferred force of each batch and the inferred force from 1000 vehicles crossing a healthy bridge. The values calculated for Axle 1 can be seen in Fig 9.

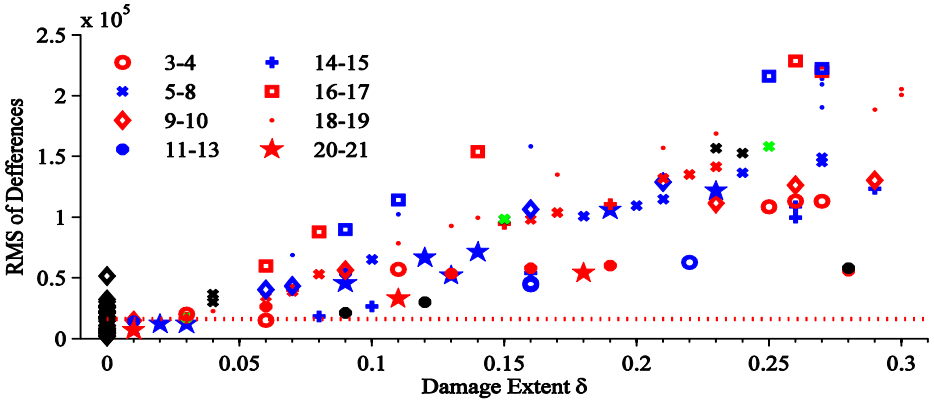


Figure 9: Damage Extent vs RMS of the differences for 100 batches of 100 trucks

Also plotted on this figure is RMS of the differences between the 1000 vehicle healthy bridge inferred force and 20 batches of 100 vehicles where $\delta = 0$. This is to illustrate the variability present in the data points. The dotted red line is the mean value of all twenty root mean squares.

Using the same data and some interpolation to estimate the values for other damage location/extent pairings a contour plot was created and is seen in Fig 10.

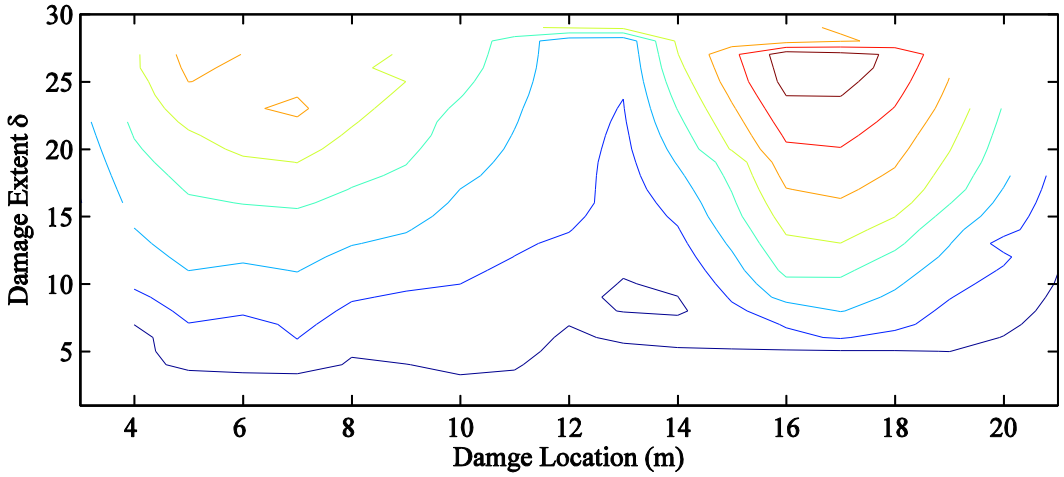


Figure 10: Contour plot of RMS of the various damage scenarios and interpolated values

To investigate the robustness of using mean inferred force as a damage indicator, a similar process was carried out with a signal to noise ratio of 10. Each batch of 100 vehicles was simulated crossing a different class A road profile. The 'healthy' force was taken as the mean of three $\delta = 0$ batches. The results of this are shown in Figure 11.

Figs. 9, 10 and 11 show a general trend of increasing deviation away from the healthy bridge inferred force as the damage extent increases. As highlighted by the twenty batches of 100 vehicles crossing the healthy bridge, there can be a significant difference between batches with the same damage location and extent. If the number of vehicles per batch were increased, errors would be expected to cancel making the RMS data points more repeatable and the trends present in this study even more evident. However, at this point in time, the method can only be claimed to be an indicator of damage and cannot guarantee reliable results in all cases. In particular, a change in road surface profile may have a similar effect to bridge damage.

The crossing events simulated here are not representative of actual bridge traffic as all events are of a single vehicle of the same type with varying properties. This approach of discarding all but one vehicle type is deliberate as it minimises the variability arising from axle weights and spacings. For long-distance freight routes where 5-axle articulated vehicles are most common, it may be best to use this type as it will be

possible to average results for greater numbers of vehicles and the heavier vehicles will excite the bridge better.

It should also be noted that if the batch of vehicles is taken over multiple days, the influence of daily temperature variations are removed but seasonal temperature effects will remain and will need to be corrected for.

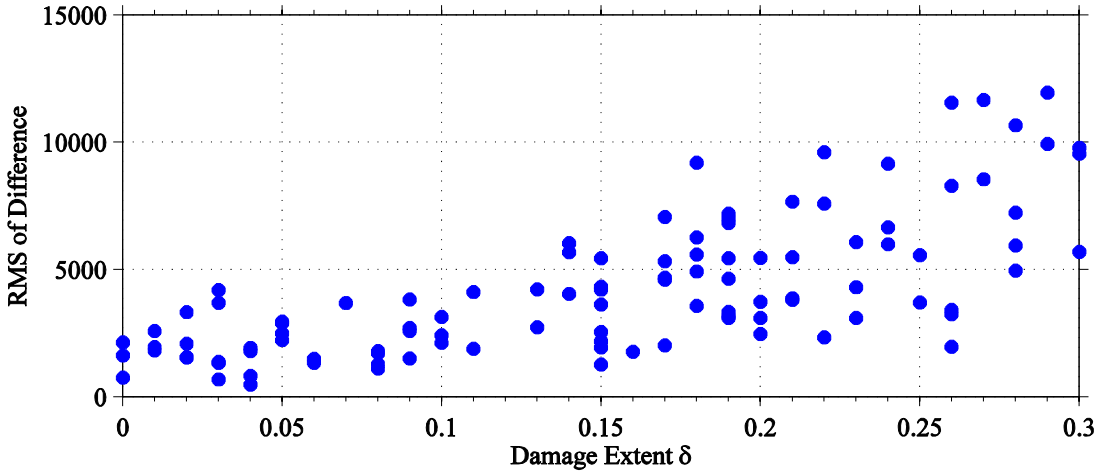


Figure 11: RMS of the differences vs damage extent for 100 batches of 100 trucks, SNR of 10

## 8. Conclusions

This paper uses an optimisation approach to find the force histories that minimise the sum of the squares of the differences between measured and theoretical deflections. This calculation of force histories is found to be highly sensitive to bridge damage. The mean inferred axle force histories for fleets of vehicles, are therefore used as damage indicators. Using the mean of a large fleet removes most of the influence of individual vehicle dynamic properties.

Signals from strain transducers, as commonly used in bridge monitoring, were investigated initially as the input signal. However results indicate that the approach is ineffective unless the sensor is close to the damage location. As an alternative to the use of strain signals, this paper investigates the use of deflection signals. Results indicate that damage can be detected in the inferred axle force histories. The axle force histories deviate more from those of the healthy bridge as damage increases. It is clear that both axles give a good indication of damage and the best results are when both axles are on the bridge.

The location of the damage plays an important role in using RMS as an indicator for damage. The results show when the damage is located near the centre of the bridge, the damage indicator is much less sensitive than when damage is off-centre.

## 9. Acknowledgements

The authors wish to acknowledge the financial support received from the Irish Research Council and Science Foundation Ireland under the US-Ireland Research Partnership Scheme towards this investigation. The authors also would like to thank the Rijkswaterstaat, the Dutch Ministry of Transport and Infrastructure, for use of their WIM data.

## References

[1] M. Azarbayejani, A. El-Osery, and M. M. Reda Taha, "Entropy-based optimal sensor networks for structural health monitoring of a cable-stayed bridge," *Smart Struct. Syst.*, vol. 5, pp. 369–379, 2009.

[2] J. Tu and M. Lindblom, "Probe of I-5 bridge collapse shifts underwater," *The Seattle Times*.

[3] E. P. Carden and P. Fanning, "Vibration Based Condition Monitoring: A Review," *Struct. Heal. Monit.*, vol. 3, no. 4, pp. 355–377, 2004.

[4] H. Sohn, C. R. Farrar, F. Hemez, D. D. Skunk, D. W. Stinemates, B. R. Nadler, and J. Czarnecki, "A Review of Structural Health Monitoring Literature: 1996–2001," Los Alamos New Mexico, 2004.

[5] S. W. Doebling, C. R. Farrar, and M. B. Prime, "A summary review of vibration based damage identification methods," *Eng. Anal.*, pp. 1–34, 1997.

[6] A. Cunha, E. Caetano, F. Magalhães, and C. Moutinho, "Recent perspectives in dynamic testing and monitoring of bridges," *Structural Control and Health Monitoring*, vol. 20, no. August 2012. pp. 853–877, 2013.

[7] O. S. Salawu, "Detection of structural damage through changes in frequency : a review," *Science (80-. ).*, vol. 19, no. 9, pp. 718–723, 1997.

[8] F. Cerda, J. Garrett, J. Bielak, P. Rizzo, J. Barrera, Z. Zhuang, S. Chen, M. McCann, and J. Kovacevic, "Indirect Structural Health Monitoring in Bridges," in *Proceedings of International Conference on Bridge Maintenance, Safety and Management*, 2012, pp. 346–353.

[9] A. Messina, E. J. Williams, and T. Contursi, "Structural Damage Detection by A Sensitivity and Statistical-Based Method," *J. Sound Vib.*, vol. 216, pp. 791–808, 1998.

[10] J. Kim and N. Stubbs, "Improved damage identification method based on modal information," *J. Sound Vib.*, vol. 252, no. 2, pp. 223–238, 2002.

[11] J. T. Kim, Y. S. Ryu, H. M. Cho, and N. Stubbs, "Damage identification in beam-type structures: Frequency-based method vs mode-shape-based method," *Eng. Struct.*, vol. 25, no. 1, pp. 57–67, 2003.

[12] H. W. Shih, D. P. Thambiratnam, and T. H. T. Chan, “Damage detection in slab-on-girder bridges using vibration characteristics,” *Struct. Control Heal. Monit.*, vol. 20, pp. 1271–1290, 2013.

[13] Williams and O. S. Salawu, “Damping as a damage indication parameter,” in *Proceedings of the 15th International Modal Analysis Conference*, 1997, pp. 1531–1536.

[14] J. Keenahan, E. J. OBrien, P. J. McGetrick, and A. Gonzalez, “The use of a dynamic truck-trailer drive-by system to monitor bridge damping,” *Struct. Heal. Monit.*, vol. 13, no. 2, pp. 143–157, 2014.

[15] R. O. Curadelli, J. D. Riera, D. Ambrosini, and M. G. Amani, “Damage detection by means of structural damping identification,” *Eng. Struct.*, vol. 30, no. 12, pp. 3497–3504, 2008.

[16] C. Modena, D. Sonda, and D. Zonta, “Damage localization in reinforced concrete structures by using damping measurements,” *Key Eng. Mater.*, 1999.

[17] A. P. Jeary, G. Chiu, and J. Wong, “Wholistic Structural Appraisal,” in *Proceedings of the eighth International Conference on Structural Safety and Reliability, ICOSSAR*, 2001, p. 144.

[18] G. Gutenbrunner, K. Savov, and H. Wenzel, “Sensitivity Studies on Damping Estimation,” in *Proceedings of the Second International Conference on Experimental Vibration Analysis for Civil Engineering Structures (EVACES)*, 2007.

[19] A. P. Jeary, “The description and measurement of nonlinear damping in structures,” *J. Wind Eng. Ind. Aerodyn.*, vol. 59, pp. 103–114, 1996.

[20] G. Kawiecki, “Modal damping measurement for damage detection,” *Smart Mater. Struct.*, vol. 10, pp. 466–471, 2001.

[21] A. C. Okafor and A. Dutta, “Structural damage detection in beams by wavelet transforms,” *Smart Materials and Structures*, vol. 9. pp. 906–917, 2000.

[22] E. Douka, S. Loutridis, and a. Trochidis, “Crack identification in beams using wavelet analysis,” *Int. J. Solids Struct.*, vol. 40, pp. 3557–3569, 2003.

[23] X. Q. Zhu and S. S. Law, “Wavelet-based crack identification of bridge beam from operational deflection time history,” *Int. J. Solids Struct.*, vol. 43, pp. 2299–2317, 2006.

[24] D. Hester and a. González, “A wavelet-based damage detection algorithm based on bridge acceleration response to a vehicle,” *Mech. Syst. Signal Process.*, vol. 28, pp. 145–166, Jul. 2011.

[25] Z. Hou, M. Noori, and R. St. Amamd, “Wavelet-Based approach for structural damage detection,” *J. Eng. Mech.*, vol. 1236, no. 7, pp. 677–683, 2000.

[26] W. W. Zhang, Z. H. Wang, and H. W. Ma, “Studies on Wavelet Packet-Based Crack Detection for a Beam under the Moving Load,” *Key Eng. Mater.*, vol. 413–414, pp. 285–290, 2009.

[27] H. Hattori, X. He, F. Catbas, H. Furuta, and M. Kawatani, “A bridge damage detection approach using vehicle-bridge interaction analysis and Neural Network technique,” in *Proceedings of the Sixth International IABMAS Conference*, 2012.

[28] J. J. Lee, J. W. Lee, J. H. Yi, C. B. Yun, and H. Y. Jung, “Neural networks-based damage detection for bridges considering errors in baseline finite element models,” *J. Sound Vib.*, vol. 280, pp. 555–578, 2005.

[29] E. J. OBrien, P. J. Mcgetrick, and a. González, “A drive-by inspection system via vehicle moving force identification,” *Smart Struct. Syst.*, vol. 13, pp. 821–848, 2014.

[30] A. Yabe and A. Miyamoto, “A. Bridge condition assessment for short and medium span bridges by vibration responses of city bus,” in *Proceedings of the Sixth International IABMAS Conference*, 2012.

[31] U. P. Poudel, G. Fu, and J. Ye, “Structural damage detection using digital video imaging technique and wavelet transformation,” *J. Sound Vib.*, vol. 286, pp. 869–895, 2005.

[32] F. Moses, “Weigh-in-Motion System Using Instrumented Bridges,” *Transp. Eng. J.*, vol. 105, no. 3, pp. 233–249, 1979.

[33] C. W. Rowley, E. OBrien, A. Gonzalez, and A. Žnidarič, “Experimental Testing of a Moving Force Identification Bridge Weigh-in-Motion Algorithm,” *Exp. Mech.*, vol. 49, no. 5, pp. 743–746, Nov. 2008.

[34] A. González, C. Rowley, and E. J. OBrien, “A general solution to the identification of moving vehicle forces on a bridge,” *Int. J. Numer. Methods Eng.*, vol. 75, no. 3, pp. 335–354, Jul. 2008.

[35] L. Yu and T. Chan, “Recent research on identification of moving loads on bridges,” *J. Sound Vib.*, vol. 305, no. 1–2, pp. 3–21, Aug. 2007.

[36] S.-S. Law and X.-Q. Zhu, *Moving Loads – Dynamic Analysis and Identification Techniques*. CRC Press, 2011.

[37] S. S. Law and Y. L. Fang, “Moving Force Identification: Optimal State Estimation Approach,” *J. Sound Vib.*, vol. 239, no. 2, pp. 233–254, Jan. 2001.

[38] D. M. Trujillo, “The direct numerical integration of linear matrix differential equations using padé approximations,” *Int. J. Numer. Methods Enginnering*, vol. 9, no. June 1973, pp. 259–270, 1975.

[39] P. Hansen, “Analysis of discrete ill-posed problems by means of the L-curve,” *SIAM Rev.*, vol. 34, no. 4, pp. 561–580, 1992.

[40] D. M. Trujillo, “Application of dynamic programming to the general inverse problem,” *Int. J. Numer. Methods Eng.*, vol. 12, pp. 613–624, 1978.

[41] R. Bellman, *Introduction to mathematical theory of control processes*. New York: Academic Press, 1967.

[42] J. . Sinha, M. . Friswell, and S. Edwards, “Simplified Models for the Location of Cracks in Beam Structures Using Measured Vibration Data,” *J. Sound Vib.*, vol. 251, no. 1, pp. 13–38, Mar. 2002.

[43] A. González and A. Žnidarič, “Recommendations on dynamic amplification allowance,” *Assess. Rehabil. Cent. Eur. Highw. Struct. ARCHES, Deliv. D10*, 2009.

[44] S. S. Law and Z. R. Lu, “Crack identification in beam from dynamic responses,” *J. Sound Vib.*, vol. 285, no. 4–5, pp. 967–987, Aug. 2005.

[45] E. J. OBrien and J. Keenahan, “Drive-by damage detection in bridges using the apparent profile,” *Struct. Control Heal. Monit.*, p. DOI: 10.1002/stc.1721., 2014.

[46] ISO8608, “Mechanical vibration-Road surface profiles-Reporting of measure data,” 1995.

[47] N. K. Harris, E. J. OBrien, and a. González, “Reduction of bridge dynamic amplification through adjustment of vehicle suspension damping,” *J. Sound Vib.*, vol. 302, no. 3, pp. 471–485, May 2007.

[48] D. Cebon, *Handbook of vehicle-road interaction*. The Netherlands: Swets & Zeitlinger, 1999.

[49] D. Cantero and A. González, “Location and Evaluation of Maximum Dynamic Effects on a Simply Supported Beam due to a Quarter-Car Mod,” in *Bridge and Concrete Research in Ireland*, 2008, pp. 119–126.

[50] C. O’Connor and T. Chan, “Dynamic wheel loads from bridge strains,” *J. Struct. Eng.*, vol. 114, no. 8, pp. 1703–1723, 1988.

[51] T. H. T. Chan, L. Yu, and S. S. Law, “Comparative Studies on Moving Force Identification From Bridge Strains in Laboratory,” *J. Sound Vib.*, vol. 235, no. 1, pp. 87–104, Aug. 2000.

[52] T. OConnor, E. J. OBrien, and B. Jacob, “An experimental investigation of spatial repeatability,” *Int. J. Heavy Veh. Syst.*, vol. 7, no. 1, pp. 64–81, 2000.

[53] Y. Yao, S. T. E. Tung, and B. Glisic, “Crack detection and characterization techniques-an overview,” *Structural Control and Health Monitoring*, p. DOI: 10.1002/stc.1655, 2014.

[54] L. Wu and F. Casciati, “Local positioning systems versus structural monitoring: A review,” *Structural Control and Health Monitoring*, vol. 21, no. January. pp. 1209–1221, 2014.

[55] B. K. Raghuprasad, N. Lakshmanan, N. Gopalakrishnan, K. Sathishkumar, and R. Sreekala, “Damage identification of beam-like structures with contiguous and distributed damage,” *Struct. Control Heal. Monit.*, vol. 20, no. March 2012, pp. 496–519, 2013.

[56] S. Q. Wu and S. S. Law, “Statistical moving load identification including uncertainty,” *Probabilistic Eng. Mech.*, vol. 29, pp. 70–78, 2012.

[57] H. Yan, Q. Chen, G. Yang, R. Xu, and M. Wang, “A Study of Inertia Force Identification by Inverse Method Between Cantilever Structure and Moving Mass,” in *Vibroengineering PROCEDIA Volume 2*, 2013, pp. 29–34.

[58] J. Tedesco, W. McDougal, and C. Ross, *Structural dynamics: theory and applications*. Addison Wesley Longman, 1999.

[59] M. F. Green and D. Cebon, “Dynamic interaction between heavy vehicles and highway bridges,” *Comput. Struct.*, vol. 62, no. 2, pp. 253–264, 1997.